

AI-Based Monitoring of Solar Panels in Desert Environments: Distinguishing Dust Accumulation for Fault Detection

Fady F. El-Batta^{1,*}  , Alsanossi M. Aboghrara²  , Rifa J. El-Khozondar³  , Hala J. El-Khozondar^{4,5}  ,
Yasser F. Nassarr⁶  

¹Electrical Appliances Department, Ministry of Health, Palestine

²Renewable Energy Department, Faculty of Engineering, Sebha University, Libya

³Physics Department, Al-Aqsa University, Gaza, Palestine

⁴Electrical Engineering and Smart Systems Department, Islamic University of Gaza, P.O. Box 108, Gaza, Palestine

⁵Department of Materials and London Centre for Nanotechnology, Imperial College London, UK

⁶Department of Mechanical and Renewable Energy Engineering, Faculty of Engineering, Wadi Alshatti University, Libya

ARTICLE HISTORY

Received 19 March 2026

Revised 02 April 2026

Accepted 12 April 2026

Online 16 April 2026

KEYWORDS

Artificial intelligence;

Image classification;

Solar cells;

Dust;

Fault monitoring;

Efficiency

ABSTRACT

Dust accumulation on photovoltaic (PV) panels in arid and desert environments poses a significant challenge by degrading conversion efficiency and reducing overall energy yield. A comparative analysis was conducted using three supervised classifiers—Logistic Regression, Support Vector Machine (SVM), and Multi-Layer Perceptron (MLP)—trained and tested on a dataset comprising 2,562 PV images (1,493 clean and 1,069 dusty) obtained from Kaggle, a widely used data science and machine learning platform. The proposed pipeline integrates robust image pre-processing steps, including resizing to 224×224 pixels, contrast enhancement via Contrast Limited Adaptive Histogram Equalization (CLAHE), and RGB normalization. Feature extraction yielded 28 engineered descriptors encompassing grayscale intensity statistics, RGB and HSV (Hue, Saturation, Value) color characteristics, edge-based morphology, and texture information. Experimental results indicate that the SVM classifier outperformed the other models, achieving a validation accuracy of 75.78% and a test accuracy of 74.07%, with balanced precision and recall values of 74.00% and 74.07%, respectively. Notably, the model demonstrated higher recall for clean panel detection (79%) compared to dusty panels (68%), highlighting the complexity associated with detecting varying degrees of soiling. Furthermore, the SVM achieved an area under the Receiver Operating Characteristic (ROC) curve of 0.790 while maintaining low computational complexity. The results demonstrate that the proposed SVM-based approach is a practical and efficient solution for automated solar panel monitoring in desert environments, enabling timely maintenance and reducing energy losses.

مراقبة الألواح الشمسية في البيئات الصحراوية باستخدام الذكاء الاصطناعي: تمييز تراكم الغبار للكشف عن الأعطال

فادي فضل البطة^{1*}، السنوسي أبوغرة²، رفعة جار الله الخزندار³، هالة جار الله الخزندار^{4,5}، ياسر فتحي نصار⁶

المخلص	الكلمات المفتاحية
يشكل تراكم الغبار على الألواح الكهروضوئية في البيئات الصحراوية تحديًا كبيرًا، إذ يُقلل من كفاءة التحويل ويُخفض من إنتاج الطاقة. تُقدم هذه الدراسة إطارًا عمليًا آليًا للكشف عن الغبار، بالاعتماد على تقنيات التعلم الآلي ورؤية الحاسوب. أُجري تحليل مقارنة باستخدام ثلاثة مصنّفات خاضعة للإشراف - الانحدار اللوجستي، وآلة المتجهات الداعمة (SVM)، والشبكة العصبية متعددة الطبقات (MLP) - تم تدريبها واختبارها على مجموعة بيانات تضم 2562 صورة للألواح الكهروضوئية (1493 صورة نظيفة و1069 صورة مغبرة) تم الحصول عليها من Kaggle، يدمج النظام المقترح خطوات معالجة مسبقة قوية للصور، تشمل تغيير حجمها إلى 224×224 بكسل، وتحسين التباين باستخدام معادلة المدرج التكراري التكيفي المحدود التباين (CLAHE)، وتطبيق قيم RGB. أسفر استخلاص الميزات عن 28 واصفًا مُهندَسًا تشمل إحصائيات شدة تدرج الرمادي، وخصائص ألوان RGB و HSV (الصبغة، التشبع، القيمة)، وشكل الحواف، ومعلومات النسيج. تشير النتائج التجريبية إلى تفوق مُصنّف SVM على النماذج الأخرى، محققًا دقة بلغت 75.78% ودقة اختبار بلغت 74.07%، مع قيم متوازنة للدقة والاستدعاء بلغت 74.00% و74.07% على التوالي. والجدير بالذكر أن النموذج أظهر استدعاءً أعلى في الكشف عن الألواح النظيفة (79%) مقارنةً بالألواح المغبرة (68%)، مما يُبرز التعقيد المرتبط بالكشف عن درجات متفاوتة من الاتساخ. علاوة على ذلك، حقق SVM مساحة تحت منحنى خصائص تشغيل المُستقبل (ROC) بلغت 0.790. تُظهر النتائج أن النهج المقترح القائم على SVM يُعد حلًا عمليًا وفعالًا للمراقبة الآلية للألواح الشمسية في البيئات الصحراوية، مما يُتيح الصيانة في الوقت المناسب ويُقلل من فقد الطاقة.	الذكاء الاصطناعي تصنيف الصور الخلايا الشمسية الغبار مراقبة الأعطال الكفاءة

*Corresponding author

https://doi.org/10.63318/waujpasv4i1_38

This work is licensed under a Creative Commons Attribution-NonCommercial 4.0 International License (CC BY-NC 4.0).



Introduction

Electricity is a cornerstone of modern economic activity and societal development; however, its predominant generation from finite fossil fuel resources, such as coal and petroleum, remains a major contributor to greenhouse gas emissions and environmental degradation. The transition toward renewable energy sources is therefore essential to achieve climate change mitigation, enhance energy security, and support sustainable development [1-4]. Among renewable energy technologies, solar photovoltaic (PV) systems—which directly convert solar radiation into electrical energy—have gained increasing prominence due to their abundant resource availability, scalability, and rapidly declining costs. Nevertheless, the conversion efficiency of commercial PV modules remains below 23%, indicating substantial potential for further improvement [5,6]. Moreover, PV system performance is adversely affected by factors such as module faults and surface dust accumulation [7], underscoring the need for effective monitoring, fault detection, and maintenance strategies to ensure reliable and sustainable power generation. The continuous growth in global energy demand further highlights the urgent need to expand clean energy capacity. Solar energy, owing to its minimal environmental footprint and ability to reduce dependence on fossil fuels, represents a viable pathway for lowering carbon emissions, preserving ecological balance, and strengthening energy independence.

As fossil fuel reserves continue to decline, research efforts have increasingly shifted toward solar energy as a sustainable alternative. This trend is particularly evident in the solar belt region, where solar resources are abundant. Consequently, intensified research activity aims to harness solar energy to meet the rising global electricity demand while mitigating environmental pollution [8–16].

Extensive investigations have examined solar energy systems operating either as standalone configurations [17–21] or as components of hybrid energy systems [22–30]. In the Middle East, exceptionally high solar irradiance levels make PV technology especially attractive, particularly in regions experiencing persistent electricity shortages [31–39]. However, the photovoltaic module, the fundamental building block of any PV system, exhibits conversion efficiency that is highly sensitive to environmental conditions such as solar irradiance, temperature variations, and partial shading [40–52]. These factors cause continuous shifts in the maximum power point (MPP) of the PV array [53,54]. Without accurate and efficient MPP tracking, a substantial portion of the available solar energy cannot be effectively harvested [55,56]. To assess the environmental impacts on photovoltaic (PV) system performance, recent research has increasingly focused on the application of artificial intelligence-based techniques.

Artificial Intelligence (AI) is concerned with the development of systems capable of performing tasks that traditionally require human intelligence, such as reasoning, learning, and problem-solving. Machine Learning (ML), a key subset of AI, is particularly well suited to addressing complex and dynamic problems in which explicit input–output relationships are not clearly defined, as it can adapt to new data without relying on extensive predefined rules [57–59].

Deep Learning (DL), a specialized branch of ML, employs multi-layered neural networks to automatically extract features from raw data, improving prediction and classification for large, complex datasets while eliminating

the need for manual feature engineering. However, conventional ML often outperforms DL in scenarios with limited data due to its lower data requirements. The selection of AI methods depends on problem type, dataset size, algorithmic complexity, implementation effort, and required performance. Hierarchically, DL is nested within ML, and ML within AI, reflecting both their interconnections and distinct capabilities (Figure 1) [60–62].

AI has revolutionized photovoltaic (PV) system optimization, enhancing energy yield, efficiency, and operational reliability. Applications include solar resource assessment, dynamic panel orientation via AI-driven tracking systems, and predictive maintenance through continuous monitoring of voltage, current, and temperature [57]. ML paradigms, supervised, semi-supervised, unsupervised, and reinforcement learning, enable tasks such as condition classification, fault detection, and adaptive energy management in PV systems [55].

Belu [58] reviewed AI applications in solar energy, highlighting neural networks, fuzzy logic, and genetic algorithms for modeling solar radiation, sizing PV systems, performance evaluation, and control. The study demonstrated that AI could provide accurate solar resource predictions even in regions with sparse data and could model auxiliary meteorological variables, such as air temperature, wind speed, and humidity. Importantly, AI was shown to be effective for optimal PV system sizing in off-grid and isolated contexts, achieving reasonable accuracy with limited datasets.

Umoh et al. [60] developed a Smart Solar Energy Management System (SSEMS) to harvest solar energy, supply loads, and store excess power in batteries. The modular system was simulated, constructed, and tested, demonstrating the ability to prioritize loads and manage battery charging/discharging according to state-of-health. This work highlighted the potential of intelligent control systems for efficient energy distribution from limited PV sources and provided a blueprint for scalable, research-oriented or industrial applications.

Habib et al. [61] introduced an Arduino-based, automatic, waterless cleaning system for dust removal on PV panels in arid regions. The system combined an air blower to displace loose dust and a DC motor-driven wiper to remove residual particles. It achieved 87–96% cleaning efficiency without surface damage, demonstrating a low-cost, water-free solution for maintaining PV performance in desert climates.

Jumaboev et al. [63] addressed production losses in large-scale solar farms using unmanned aerial vehicle (UAV)-based thermal imaging for automated fault detection. They evaluated three deep learning semantic segmentation models—DeepLabV3+, Feature Pyramid Network (FPN), and U-Net—with intersection over Union (IoU) scores of 79–86% and dice coefficients of 87–94%. The study demonstrated that UAV-assisted deep learning provides scalable and accurate PV fault detection, overcoming limitations of manual inspections.

Duranay [64] applied deep learning for defect detection using 20,000 infrared images of PV panels across 12 defect classes (e.g., cracking, hot spots, soiling). The approach employed EfficientNetb0 for feature extraction, Neighborhood Component Analysis (NCA) for feature selection, and SVM for classification, achieving 93.93% accuracy and robust precision, sensitivity, and F1-scores. This work highlighted the effectiveness of hybrid DL-SVM pipelines for automated defect detection.

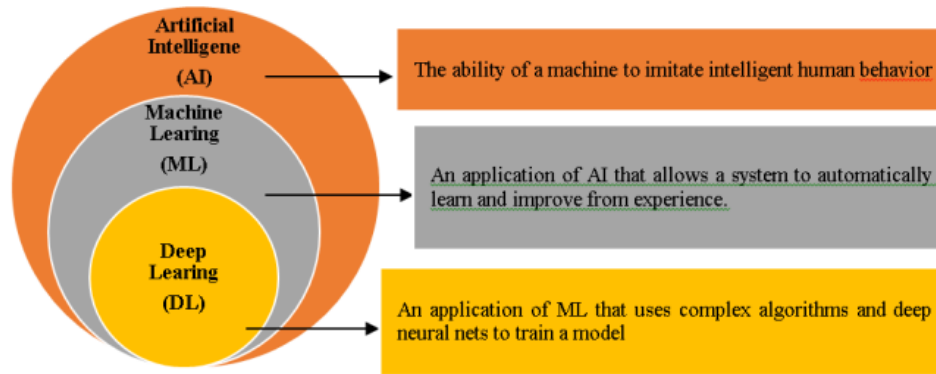


Figure 1: The connections between AI, ML, and DL

Alatwi et al. [65] focused on detecting dust accumulation on PV panels using image classification. Twenty pre-trained deep learning models were evaluated, and DenseNet169 with a linear SVM achieved the highest accuracy (86.79%). By leveraging existing surveillance camera images, the approach eliminated the need for additional sensors, demonstrating a practical and scalable method for automated dust detection.

Kechida et al. [66] proposed a smart hybrid energy management system integrating PV, wind, battery storage, and AC/DC loads. ANFIS-based MPPT techniques achieved 99.7% PV and 98% wind efficiency, outperforming conventional methods. A PI-ANFIS controller maintained stable DC bus voltage under variable solar, wind, and load conditions, while fuzzy logic-based energy management prioritized loads based on battery state-of-charge, solar irradiance, and wind speed, ensuring optimal energy utilization.

Mamodiya et al. [67] introduced a multi-layer AI-enhanced hybrid solar framework integrating CNN-LSTM for irradiance prediction, reinforcement learning for dual-axis tracking, and Edge AI for low-latency decision-making. Advanced materials (self-cleaning nanocoatings, phase-change materials, adaptive perovskite-silicon cells) and a blockchain-enabled smart grid enabled secure energy trading. Field testing showed a 41.4% increase in annual energy yield, an 11.9 °C reduction in average panel temperature, and a 60% extension of battery lifespan.

Karthik et al. [68] developed a unified deep learning platform for simultaneous dust and fault detection using CNN, ResNet, and self-attention KerNet models. The system included preprocessing steps such as gamma correction and Gaussian filtering and achieved high accuracy, precision, and F1 scores, supporting real-time, scalable deployment from residential to utility-scale PV systems.

Lin et al. [6] reviewed the integration of AI, IoT, and big data analytics for PV optimization, emphasizing predictive maintenance, real-time monitoring, and energy forecasting. The synergy of these technologies maximizes energy harvesting, reduces operational costs, and enhances grid stability, positioning smart PV systems as central to resilient, sustainable energy infrastructures.

Building on this body of work, the present study focuses on developing a machine learning-based classification model to autonomously detect solar panel surface conditions (clean vs. dirty) from annotated images. By providing a data-driven decision-support tool for maintenance scheduling, this research aims to mitigate energy yield losses caused by soiling. Multiple classification algorithms—Logistic

Regression, SVM, and MLP—were implemented and rigorously compared using standardized performance metrics to identify the most effective approach for this computer vision task. This study contributes to bridging AI methodologies with practical PV system maintenance, enhancing operational efficiency and reliability.

Novelty

The novelty of this work lies in the **comparative analysis of three distinct classification algorithms** for automated visual inspection of solar panels. The problem was formulated as a **binary classification task**, distinguishing between clean and dirty panels. A **feature-based approach** was employed, extracting approximately 28 discriminative features from each image to serve as inputs for the three algorithms. Unlike prior studies that rely solely on deep learning or complex hybrid pipelines, this work emphasizes a **data-driven, interpretable framework** that balances computational efficiency, accuracy, and scalability. By systematically evaluating the performance of multiple classifiers on the same feature set, this study provides insights into the **most suitable machine learning approach for real-time PV maintenance applications**, offering a practical, implementable solution for improving energy yield.

Definitions

Logistic Regression is a statistical classification method that models the probability of a binary outcome by applying the logistic (sigmoid) function to a linear combination of input features. It assumes a linear relationship between the predictors and the log-odds of the response variable, allowing the output to be interpreted as a probability between 0 and 1. The model coefficients provide insight into the influence of each feature on the outcome, making Logistic Regression both interpretable and computationally efficient. Although primarily designed for binary classification, it can be extended to multiclass problems using multinomial or one-vs-rest strategies [69].

Support Vector Machine (SVM) is a supervised learning algorithm that constructs an optimal separating hyperplane by maximizing the margin between data points of different classes. The samples that lie closest to the decision boundary, known as support vectors, determine the model structure. For non-linearly separable data, SVM employs kernel functions to project inputs into higher-dimensional spaces, enabling complex decision boundaries. SVM is particularly effective in high-dimensional feature spaces and is widely used in applications such as text classification, image recognition, and bioinformatics [70]

Multi-Layer Perceptron (MLP) is a feedforward artificial

neural network (ANN) consisting of an input layer, one or more hidden layers, and an output layer, with fully connected neurons. Each neuron applies a non-linear activation function to a weighted sum of its inputs, enabling the network to learn complex, non-linear relationships. The model is trained using backpropagation to minimize a loss function. MLPs are powerful for classification and regression tasks but typically require large datasets and offer limited interpretability compared to simpler models. While highly predictive, the internal reasoning is often less interpretable than Logistic Regression or SVM. Applied to a vast range of problems, including complex classification, regression, and as a building block in modern deep learning architectures [71].

Methodology and Results

In this study, a solar panel dust detection model was developed using the Python programming language, following a structured machine learning pipeline, as illustrated in Figure 3. The workflow consists of six main stages.

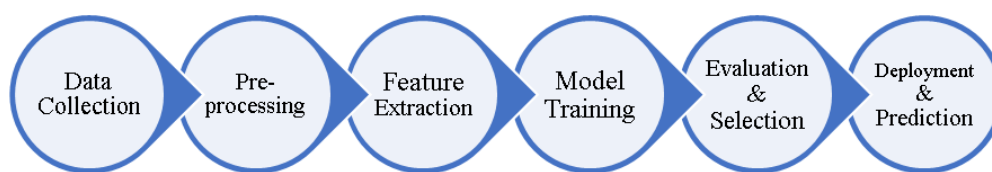


Figure 3: Solar panel dust detection flowchart

Data collection

Publicly available repositories such as Kaggle [72] provide standardized benchmark datasets that facilitate reproducible research in computer vision and machine learning. In this study, a photovoltaic (PV) panel image dataset was obtained from Kaggle, comprising 2,562 images captured under diverse environmental and operational conditions. The dataset is structured for binary classification into two categories: Clean, consisting of 1,493 images of unobstructed PV module surfaces, and Dusty, consisting of 1,069 images exhibiting visible dust or particulate accumulation.

This distribution results in a moderate class imbalance, with approximately 40% more samples in the Clean class. Since class imbalance can bias model learning and evaluation, stratified sampling and class-aware performance assessment

1. Data Collection: Image data were collected from categorized Clean and Dusty folders.
2. Preprocessing operations, including image resizing, normalization, and Contrast Limited Adaptive Histogram Equalization (CLAHE), were applied to enhance visual quality and standardize the input data.
3. Feature extraction: 28 discriminative features were extracted to characterize dust-related patterns on the panel surfaces.
4. Model training: All three classification models were then trained using the extracted features.
5. Evaluation and Selection: Model performance was evaluated through comprehensive quantitative metrics and visual analysis to identify the most effective approach.
6. Deployment & Prediction: The trained models were saved and deployed to enable real-time dust detection and performance prediction.

were employed. The images were collected through web scraping, which inherently contributed to the observed imbalance. The primary objective of using this dataset is to benchmark and compare multiple machine learning classifiers for automated dust detection on solar panels and to identify the model that achieves the highest classification performance for this task [72].

For model development and evaluation, the dataset was partitioned using stratified sampling into training (60%), validation (20%), and test (20%) subsets, thereby preserving class proportions across all splits. This configuration ensures sufficient data for learning while maintaining independent subsets for unbiased model selection and final performance evaluation. Representative samples from the training dataset are shown in Figure 4.



Figure 4: Sample training images illustrating clean and dust-affected photovoltaic panel surfaces

Image Pre-processing

Image pre-processing is a critical stage that transforms raw data into a standardized and numerically stable form suitable for machine learning. A unified pre-processing pipeline was applied to prepare the dataset for three classifiers: Support Vector Machine (SVM), Logistic Regression, and Multi-Layer Perceptron (MLP), with particular attention to normalization and scale sensitivity.

All images were resized to 224×224 pixels to ensure uniform spatial dimensions and to reduce computational complexity. Images were then converted from the BGR color space (OpenCV default) to RGB, followed by intensity normalization from the integer range $[0,255]$ to the floating-point range $[0,1]$, improving numerical conditioning and training stability.

To enhance dust-related visual cues, Contrast Limited Adaptive Histogram Equalization (CLAHE) was applied to emphasize local contrast while suppressing noise amplification. This step improves the visibility of dust-induced photometric variations without introducing artificial artifacts.

For SVM and Logistic Regression, extracted feature vectors were standardized using z-score normalization to enforce zero mean and unit variance, a requirement for classifiers sensitive to feature scale. The MLP operated directly on normalized pixel representations, with optional batch normalization applied within the network architecture. Stratified sampling was maintained during data splitting to mitigate bias caused by class imbalance.

Feature Extraction

Each solar panel image is represented by a compact set of 28 engineered features, as summarized in Table 1, designed to capture discriminative photometric, chromatic, structural, and textural characteristics that differentiate clean and dusty panels. This hand-crafted feature representation enables efficient learning while retaining sensitivity to dust-induced visual alterations.

Statistical descriptors were computed from grayscale, RGB, and HSV color spaces. The mean pixel intensity, representing overall image brightness, is defined as [73]

$$\mu = \frac{1}{N} \sum_{i=1}^N x_i \quad (1)$$

where x_i denotes the intensity of the i -th pixel and N is the total number of pixels. Image contrast and intensity dispersion were quantified using the standard deviation σ and variance σ^2 , with variance defined as [74].

$$\sigma^2 = \frac{1}{N} \sum_{i=1}^N (x_i - \mu)^2 \quad (2)$$

Additional robust measures, including the median, minimum, maximum, and first and third quartiles, were included to characterize intensity distribution asymmetry and mitigate sensitivity to outliers. Edge morphology features were extracted using Canny-based edge detection to quantify boundary density and structural complexity. Texture characteristics were captured using Laplacian-based descriptors, which measure high-frequency content degradation associated with dust-induced blurring.

Dimensionality Reduction and Dataset Representation:

The engineered feature vector reduces the original image dimensionality from 150,528 pixels ($224 \times 224 \times 3$) to 28 features, corresponding to a 99.98% reduction, while preserving photometrically relevant information for dust discrimination. The resulting dataset structure is summarized in Table 2, with all splits maintaining consistent feature dimensionality. This compact representation yields a favorable sample-to-feature ratio of approximately 55:1 in the training set, significantly reducing overfitting risk and supporting stable classifier generalization. Empirically, the extracted features form a near-linearly separable manifold for clean and dusty samples, enabling effective classification using support vector machines.

Photometric Interpretation of Features: Figure 5 illustrates the feature extraction process for a clean solar panel. Clean panels exhibit baseline photometric signatures characterized by higher grayscale mean intensity (129.75), dominant red-channel reflectance (121.47), and moderate edge density (0.3285), reflecting uniform surfaces with minimal textural disruption.

In contrast, Figure 6 shows feature extraction results for a dusty panel, revealing systematic photometric alterations induced by particulate accumulation. Grayscale luminance is attenuated (mean = 117.68), corresponding to a 9.3% reduction in reflected intensity due to dust-induced optical scattering. RGB analysis indicates wavelength-dependent extinction, with pronounced attenuation in the blue channel (-36.25), consistent with scattering by fine mineral particulates. Edge density increases slightly (0.3346), reflecting micro-edge formation caused by dust granularity, while Laplacian variance decreases, indicating loss of high-frequency detail due to surface blurring.

Table 1: The complete feature taxonomy and dimensionality

Category	Features Count	Specific Features	Explanation
Grayscale Statistics	8	mean, standard deviation, variance, minimum, maximum, median, first and third quartile (Q1, Q3)	Extracts statistical measures from the grayscale (intensity) version of the image. These capture overall brightness, contrast, and distribution of pixel intensities.
RGB Statistics	9	$R_{\text{mean}}, R_{\text{std}}, R_{\text{var}}, G_{\text{mean}}, G_{\text{std}}, G_{\text{var}}, B_{\text{mean}}, B_{\text{std}}, B_{\text{var}}$	mean, standard deviation, and variance for each color channel, capturing wavelength-dependent reflectance variations.
HSV Statistics	6	$H_{\text{mean}}, H_{\text{std}}, S_{\text{mean}}, S_{\text{std}}, V_{\text{mean}}, V_{\text{std}}$	mean and standard deviation of hue, saturation, and value, separating chromatic information from luminance in a perceptually meaningful space.
Edge Features	3	edge pixel density, mean gradient magnitude, and gradient standard deviation	Analyzes the image's edge map. Edge density is the proportion of edge pixels, indicating texture complexity. Edge mean/std describes the average intensity and variation of those edge pixels.
Texture Features	2	Laplacian variance, Laplacian mean	Uses the Laplacian filter, which is sensitive to areas of rapid intensity change (like edges and fine details). The variance and mean of the filtered image serve as quantitative measures of the panel's surface texture and granularity.

Table 2: Number of features

Dataset Split	Number of Samples	Feature Dimensions
Training Set	1,537 images	28 features
Validation Set	512 images	28 features
Test Set	513 images	28 features
Total Dataset	2,562 images	28 features

Comparative Feature Analysis: A quantitative comparison of representative clean and dusty panel features is presented in Table 3. Luminance metrics show significant attenuation (grayscale mean difference: -12.07) accompanied by increased variance ($+561.83$), suggesting non-uniform dust deposition. Spectral features exhibit wavelength-dependent

extinction, with blue-channel attenuation exceeding that of red and green channels, consistent with Rayleigh-dominated scattering. Hue mean shifts markedly (-41.53), indicating chromatic transitions toward yellow-brown tones associated with iron oxide-rich dust. Edge density and texture variance display modest increases, confirming that dust primarily affects fine-scale surface texture rather than large structural boundaries. Collectively, these complementary photometric, chromatic, and textural descriptors establish a robust multi-modal representation of dust-induced visual degradation. The resulting 28-dimensional feature space provides sufficient discriminatory power for reliable clean-versus-dusty classification while maintaining computational efficiency.

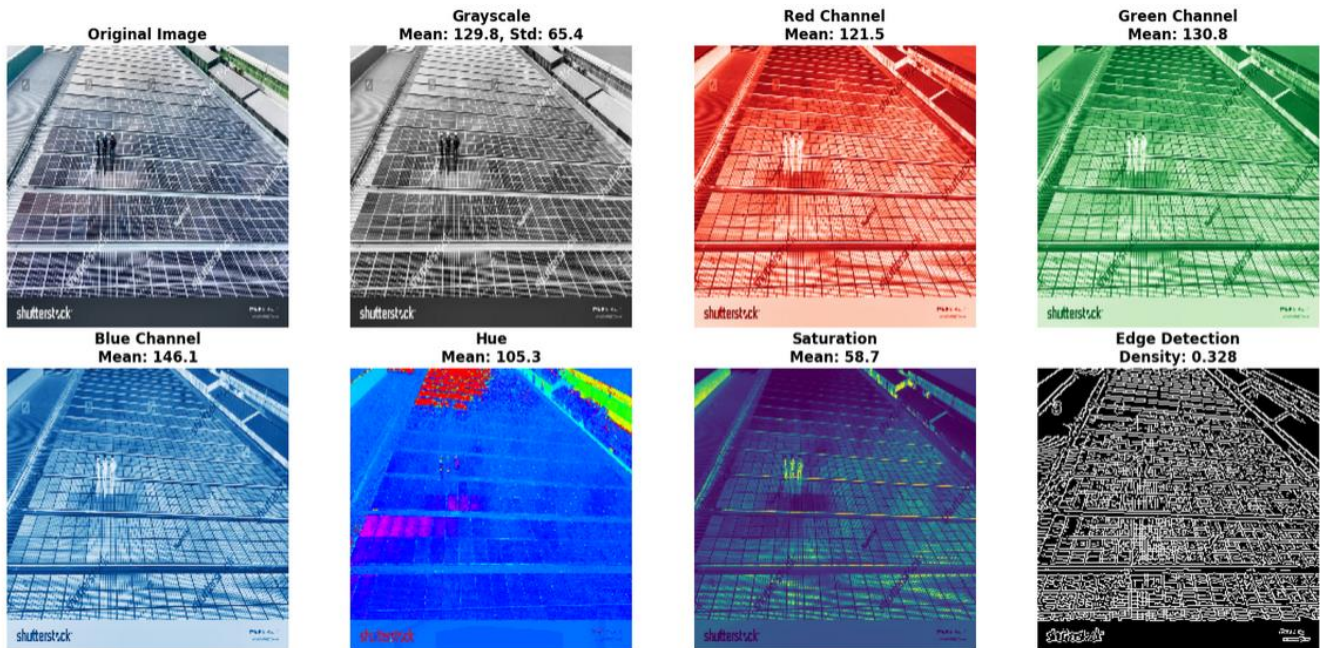


Figure 5: Illustration of extracted photometric, edge, and texture features for a clean photovoltaic panel

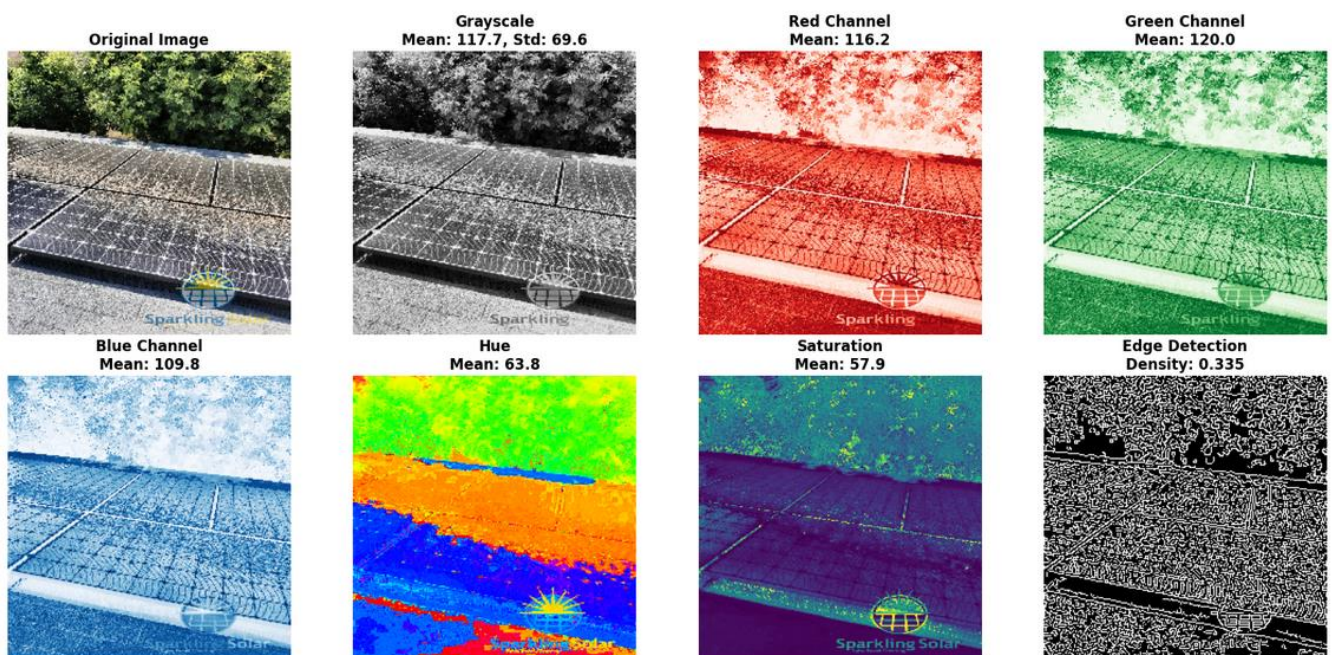


Figure 6: Illustration of extracted photometric, edge, and texture features for a dusty photovoltaic panel

Model Performance Evaluation

Three machine learning classifiers—Logistic Regression, Support Vector Machine (SVM) with a radial basis function (RBF) kernel, and Multi-Layer Perceptron (MLP)—were evaluated for photovoltaic panel dust classification using the engineered photometric feature vectors. The comparative performance results are summarized in Table 4.

Logistic Regression establishes a linear baseline, achieving a validation accuracy of 73.44%, indicating moderate discriminative capability despite the non-linear nature of dust-induced photometric variations. The MLP yields comparable performance (73.24%), suggesting that the

engineered feature space already captures near-linearly separable class structure, limiting the benefit of deeper hierarchical representations.

The SVM with RBF kernel achieves the highest validation accuracy (75.78%), demonstrating superior capability in modeling non-linear decision boundaries within the 28-dimensional feature space. Its balanced precision (76.08%) and recall (75.78%) indicate robust generalization with minimal bias toward false positives or false negatives, while the corresponding F1-score (75.87%) reflects consistent performance across classification thresholds (Figure 7).

Table 3: Comparison of extracted features for clean and dusty photovoltaic panels

Feature	Clean	Dusty	Difference
Grayscale Mean	129.75	117.68	-12.07
Grayscale Std	65.44	69.60	4.16
Grayscale Var	4281.80	4843.64	561.83
R _{mean}	121.47	116.18	-5.29
G _{mean}	130.79	119.96	-10.83
B _{mean}	146.06	109.80	-36.25
H _{mean}	105.35	63.82	-41.53
S _{mean}	58.73	57.95	-0.79
V _{mean}	146.58	125.17	-21.41
Edge Density	0.33	0.33	0.01
Texture Variance	83.76	85.32	1.56

Table 4: Model performance comparison on the validation set

Classifier	Validation			
	Accuracy (%)	Precision (%)	Recall (%)	F1-Score (%)
Logistic Regression	73.44	73.60	73.44	73.50
Support Vector Machine	75.78	76.08	75.78	75.87
Multi-Layer Perceptron	73.24	73.05	73.24	72.83

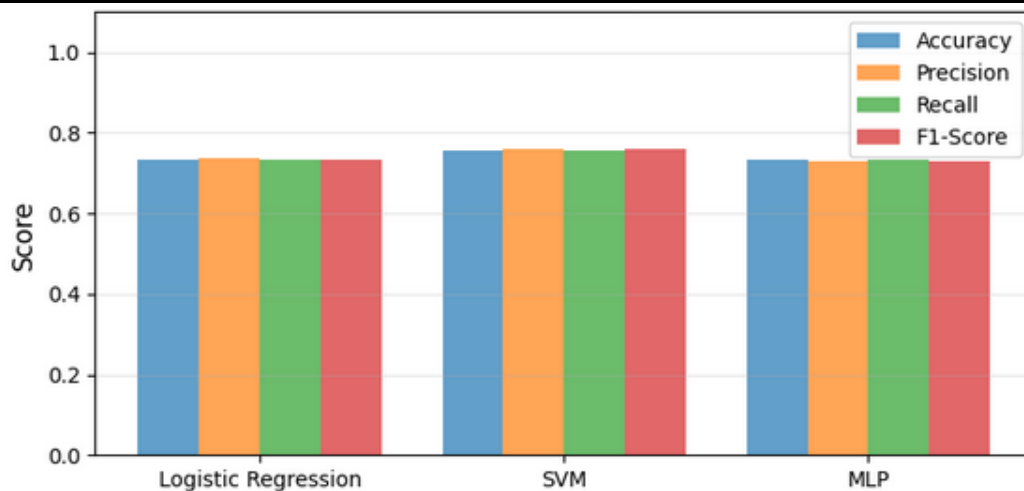


Figure 7: Validation accuracy, precision, recall, and F1-score for Logistic Regression, SVM, and MLP

Confusion Matrix Analysis:

A confusion matrix (Table 5) provides a detailed breakdown of true positives (TP), true negatives (TN), false positives (FP), and false negatives (FN) for the binary classification task [74]:

Table 5: confusion matrix

	Actual Positive (Dirty)	Actual Negative (Clean)
Predicted Positive (Dirty)	TP	FP
Predicted Negative (Clean)	FN	TN

- True Positive (TP): Dusty panels correctly classified, e.g., a dusty panel was correctly classified as "dirty".

- True Negative (TN): Clean panels correctly classified, e.g., a clean panel was correctly classified as "clean".
- False Positive (FP): Type I Error: Clean panels misclassified as dusty, e.g., a clean panel was mistakenly flagged as "dirty" (A false alarm).
- False Negative (FN): Type II Error: Dusty panels misclassified as clean, e.g., a dusty panel was missed and classified as "clean" (A missed detection).

Validation accuracy is defined as [75,76]:

$$\text{Accuracy} = \frac{N_{\text{correct}}}{N_{\text{val}}} \tag{3}$$

where N_{correct} denotes the number of correctly classified validation samples and N_{val} is the total number of validation samples. For the Dusty class, precision and recall are

computed as [75,76]

$$\text{Precision} = \frac{TP}{TP + FP} \tag{4}$$

$$\text{Recall} = \frac{TP}{TP + FN} \tag{5}$$

The F1-score, representing the harmonic mean of precision and recall, is given by [75,76]

$$\text{F1-score} = \frac{2 \cdot \text{Precision} \cdot \text{Recall}}{\text{Precision} + \text{Recall}} \tag{6}$$

The complexity-performance analysis reveals critical trade-offs between computational efficiency and classification efficacy.

Computational Complexity and Trade-off Analysis: A complexity-performance analysis highlights the trade-offs between classification accuracy and computational cost (Figures 8 and 9). Logistic Regression exhibits the lowest computational overhead (0.5× baseline training time), converging rapidly on the 28-dimensional feature space but at

the cost of reduced accuracy.

The SVM incurs moderate computational cost (2.0× baseline) while delivering the highest classification accuracy (75.78%), representing a favorable balance between discrimination capability and processing efficiency. In contrast, the MLP exhibits the highest computational burden (5.0× baseline) with no corresponding performance gain, reinforcing that increased architectural complexity yields diminishing returns for this feature representation.

The inverse relationship between training time and validation accuracy—particularly the comparison between SVM and MLP—indicates diminishing marginal utility of deep models in this context. Consequently, the SVM emerges as the Pareto-optimal solution, offering superior accuracy with acceptable computational cost, making it well suited for deployment in resource-constrained solar panel monitoring systems.

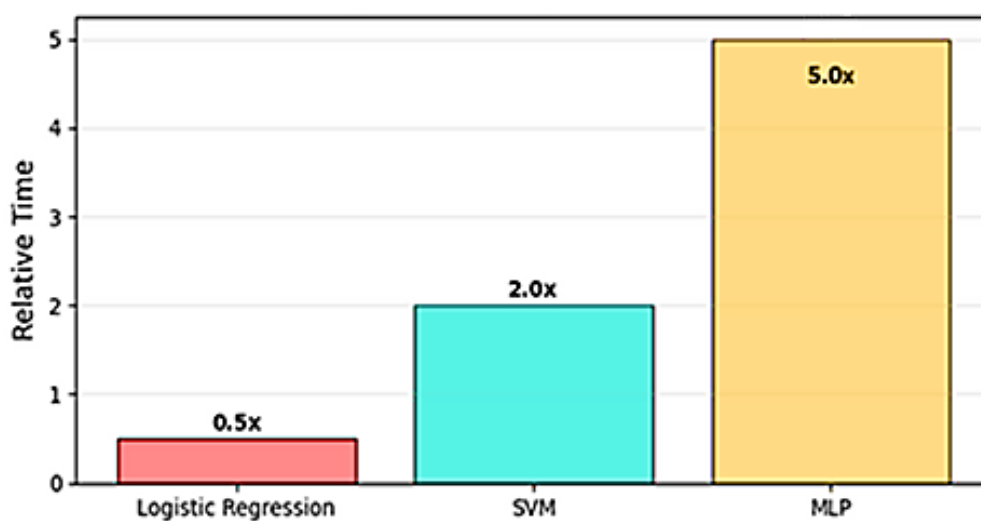


Figure 8: Training time analysis for Logistic Regression, SVM, and MLP

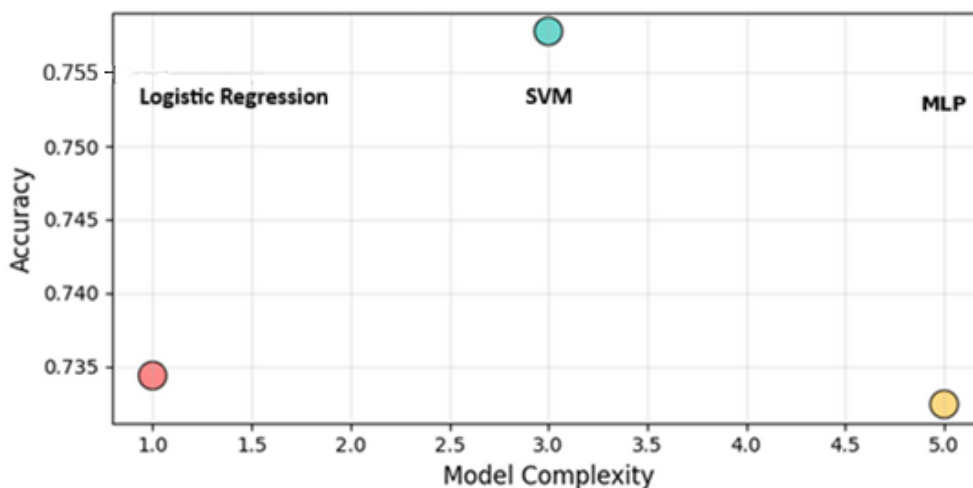


Figure 9: Trade-off between classification accuracy and computational complexity

Evaluation and Model Selection

The Support Vector Machine (SVM) demonstrates robust generalization on unseen solar panel images, achieving 74.07% test accuracy with balanced precision (74.00%) and recall (74.07%) (Figure 10). The harmonic F1-score of 74.03% confirms optimized

discrimination thresholds for the binary classification task as in figure 11. Class-specific performance reveals stronger detection of clean panels (precision: 77%, recall: 79%, F1: 78%) compared to dusty panels (precision: 69%, recall: 68%, F1: 69%), indicating that dust accumulation introduces greater photometric variability. The slight reduction in

SVM Performance on Test Set:	
✓ Accuracy:	0.7407 (74.07%)
✓ Precision:	0.7400
✓ Recall:	0.7407
✓ F1-Score:	0.7403

Figure 10: Test performance metrics of the SVM classifier

accuracy from validation (75.78%) to test (74.07%) reflects an acceptable generalization error, consistent with expected real-world variability in environmental conditions, solar angles, and dust composition. Analysis of a random test subset (12 samples) demonstrates 66.7% accuracy (8/12 correct) (Figure 12). Among the four misclassifications, three were false positives (clean panels classified as dusty), and one was a false negative (dusty panel classified as clean). This 3:1 ratio indicates a conservative bias toward dust detection, favoring preventive maintenance

Classification Report:				
	precision	recall	f1-score	support
Clean	0.77	0.79	0.78	299
Dusty	0.69	0.68	0.69	214
accuracy			0.74	513
macro avg	0.73	0.73	0.73	513
weighted avg	0.74	0.74	0.74	513

Figure 11: Classification report for SVM by class

over missed soiling events—a defensible strategy for photovoltaic monitoring. Confidence scores ranged from 47.9% to 78.5%, reflecting calibrated uncertainty rather than overconfident errors. Overall, the SVM shows deployment-ready performance, balancing clean panel reliability (79% recall) with moderate dusty panel detection (68% recall), achieving practical utility for automated solar farm monitoring.

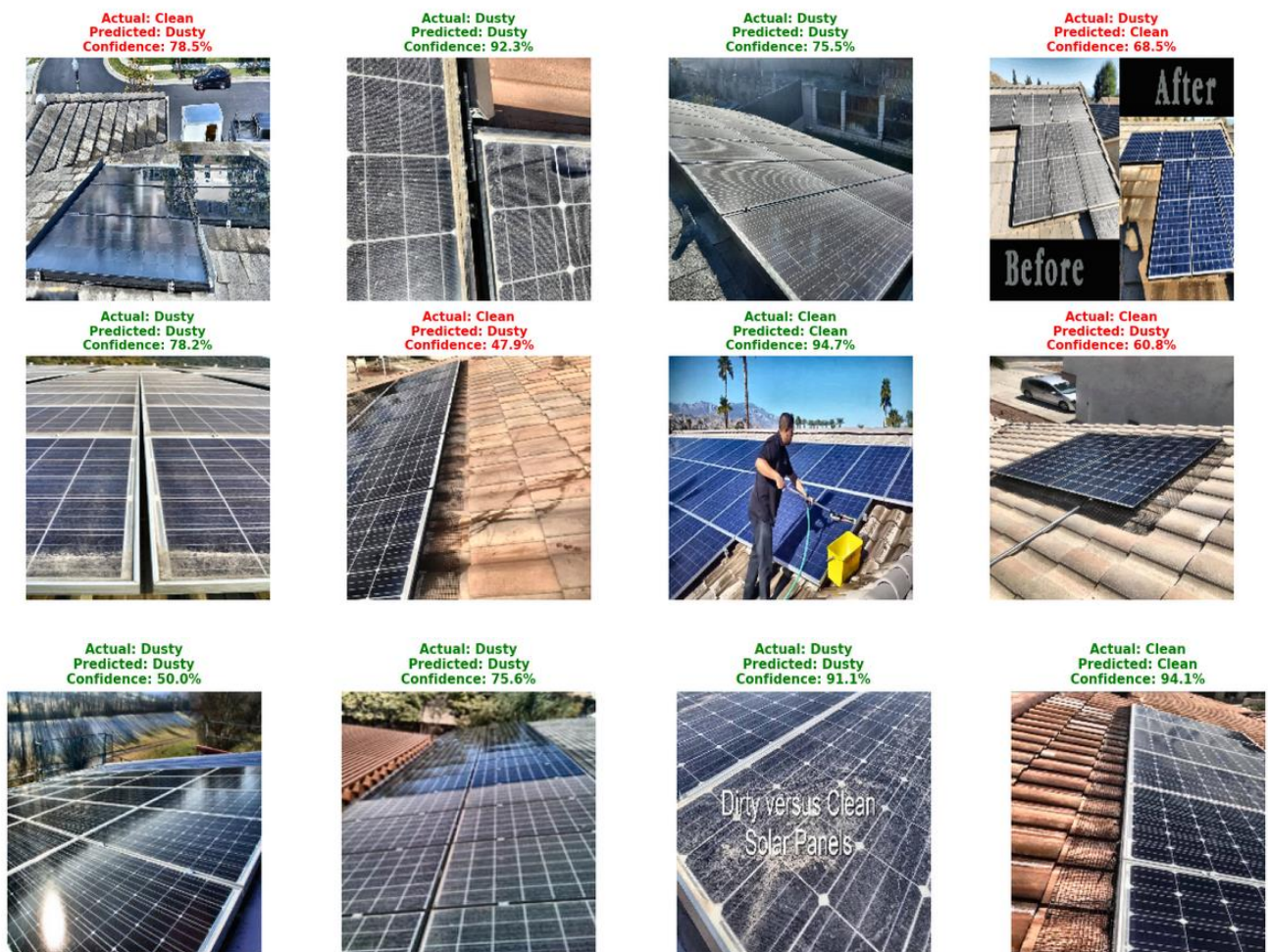


Figure 12: Random test samples: actual vs predicted labels (green color indicates correct prediction, red color indicates false prediction)

Figure 13 shows the confusion matrix for the 12-sample subset, revealing strong diagonal dominance for clean panels and more dispersed predictions for dusty panels. The asymmetric errors suggest model conservatism toward dust detection, likely influenced by feature similarity between lightly soiled and clean panels. Clean panel sensitivity reaches approximately 85%, while precision is lower (~70%), and dusty panels show the inverse pattern. Figure 14.

Displays the confusion matrix of SVM on the full test set. Across the full test set, the SVM achieves superior clean panel detection (235 TP vs. 64 FP) compared to dusty panel identification (145 TP vs. 69 FN), confirming a conservative maintenance-oriented bias.

Receiver Operating Characteristic (ROC) and Area Under Curve (AUC) Analysis: The Receiver Operating Characteristic (ROC) curve illustrates the trade-off between

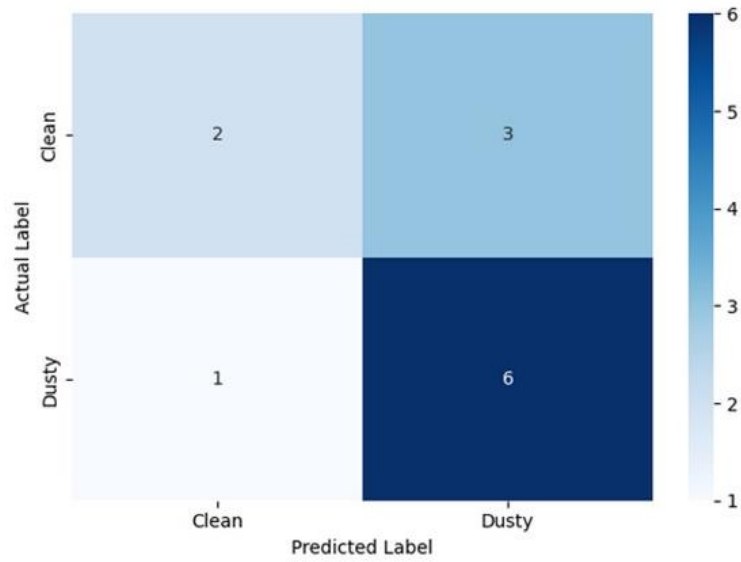


Figure 13: Confusion Matrix of test samples

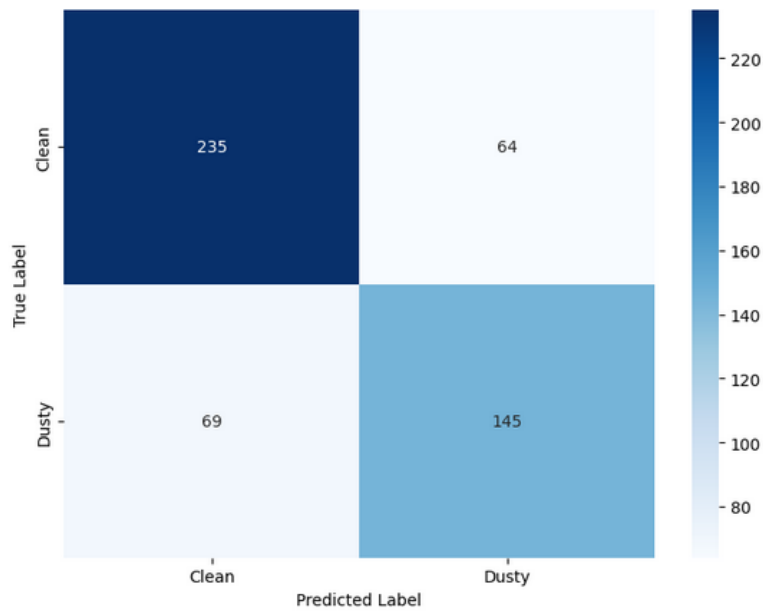


Figure 14: Confusion matrix of SVM on the full test set

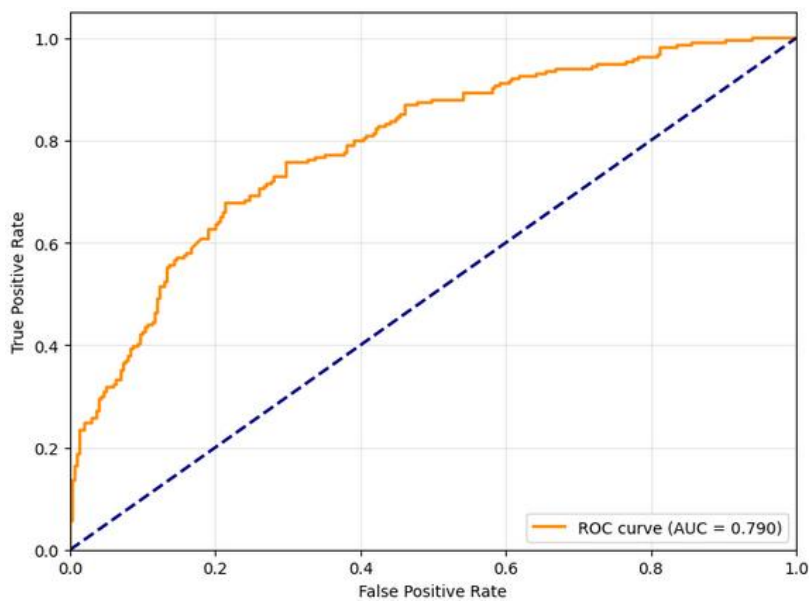


Figure 15: ROC curve for SVM

true positive rate (recall) and false positive rate across classification thresholds [12]. The Area Under Curve (AUC) is 0.790 (Figure 15), indicating good, though not perfect, separability. Optimal operating points correspond to 65–70% true positive rate with <25% false positive rate, reflecting practical deployment conditions where continuous dust gradients and environmental variability limit perfect discrimination. The asymmetric confusion matrix and gradual ROC ascent indicate overlapping feature distributions, confirming that dust accumulation is a continuum rather than a strict binary phenomenon. Despite these challenges, the SVM achieves 74.07% overall test accuracy, representing a robust, practically deployable solution for automated solar panel monitoring with real-world reliability and efficiency.

Deployment & Prediction

The optimized SVM model was serialized and deployed as the central inference component of an automated monitoring system. Within the operational workflow, incoming images undergo the same pre-processing and feature extraction procedures used during training, producing a 28-dimensional feature vector that is subsequently evaluated by the classifier to generate a real-time Clean/Dusty prediction along with an associated confidence score. This probabilistic output supports confidence-driven alerting and informed maintenance scheduling. Owing to its computational efficiency, the model enables low-latency inference and is well-suited for both edge-based and centralized deployments, thereby supporting proactive and efficient operational management.

Conclusion

This study presents a comprehensive framework for automated dust detection on photovoltaic (PV) panels using engineered photometric, chromatic, and textural features combined with machine learning classifiers. A dataset of 2,562 solar panel images, categorized as clean or dusty, was pre-processed, normalized, and transformed into a 28-dimensional feature space, enabling efficient and discriminative representation of dust-induced visual changes. Feature extraction incorporated multi-modal descriptors, including grayscale and color statistics, edge metrics, and Laplacian-based texture measures, providing robust differentiation between clean and dust-affected panels.

Three machine learning architectures—Logistic Regression, Support Vector Machine (SVM), and Multi-Layer Perceptron (MLP)—were evaluated. The SVM with a radial basis function kernel achieved the highest performance, with 74.07% test accuracy, balanced precision and recall (~74%), and an F1-score of 74.03%. Confusion matrix and ROC analyses demonstrated reliable clean panel detection, moderate dust panel identification, and an AUC of 0.790, indicating good separability despite inherent variability in environmental and operational conditions. Computational analysis highlighted the SVM as a Pareto-optimal solution, balancing classification efficacy with moderate training cost. In contrast, more complex architectures such as the MLP yielded minimal performance gain at higher computational overhead.

The proposed approach offers a practically deployable solution for solar farm monitoring, providing substantial improvements over manual inspections in terms of accuracy, consistency, and computational efficiency. While binary classification of dust presents challenges due to continuous soiling gradients, the multi-modal feature set and SVM classifier enable effective detection of significant dust

accumulation, supporting timely maintenance interventions and energy yield preservation.

Future work may explore regression-based dust quantification, multi-class soiling severity estimation, and integration with real-time aerial imaging systems, further enhancing the scalability and operational utility of automated PV monitoring frameworks.

Author Contributions: H. El-Khozondar: Conceptualization, Supervision. El-Batta and R. El-Khozondar: Methodology, Investigation, Writing – original draft. H. El-Khozondar and Nassar: Formal analysis, Software, Validation, Data curation, Writing – review & editing. All authors have read and agreed to the published version of the manuscript.

Funding: “This research received no external funding.”

Data Availability Statement: “The datasets used and/or analysed during the current study available from the corresponding author on reasonable request.”

Conflicts of Interest: “The authors declare no conflict of interest.”

References

- [1] M. Salem, et al. "Technical and environmental cost-benefit analysis of strategies towards a green economy in the electricity sector in Libya." *Economics and Policy of Energy and the Environment*, vol. 2, no. (2025/2), pp. 133-167, 2025. <https://doi.org/10.3280/EFE2025-002007>
- [2] K. Moumani. "Management of sustainable development in the light of Arab and international cooperation, a case study of the Arab vision of management of sustainable development." *Wadi Alshatti University Journal of Pure and Applied Sciences*, vol. 1, no. 1, pp. 1-8, 2023. https://doi.org/10.63318/waujpasv1i1_01
- [3] M. Khaleel, et al. "Towards Sustainable Renewable Energy." *Appl. Sol. Energy*, vol. 59, pp. 557–567, 2023. <https://doi.org/10.3103/S0003701X23600704>
- [4] S. Rekik, et al. "Towards Green Economy: : Case of Electricity Generation Sector in Libya." *Solar Energy and Sustainable Development Journal*, vol. 14, no. 1, pp. 334–360, 2025. <https://doi.org/10.51646/jesed.v14i1.549>
- [5] I. Imbayah, et al. "Modeling A 600 MW Floating Photovoltaic System in Al-Khums city, Libya: Performance Analysis and Implementation Using PVSystem." *Wadi Alshatti University Journal of Pure and Applied Sciences*, vol. 4, no. 1, 223-237, 2026. https://doi.org/10.63318/waujpasv4i1_24
- [6] C. Lin. "Enhancing energy efficiency in photovoltaic systems through smart technology integration: Innovations and future perspectives," *E3S Web Conf.*, vol. 606, p. 05004, 2025. <https://doi.org/10.1051/e3sconf/202560605004>
- [7] H. Abdulgader, et al. "Mitigation of Dust Impact on Solar Photovoltaics Performance Considering Libyan Climate Zone: A Review." *Wadi Alshatti University Journal of Pure and Applied Sciences*, vol. 1, no. 1, p. 22-27, 2023. <https://waujpas.com/index.php/journal/article/view/7>
- [8] B. Ahmed, et al. "Optimal design of hybrid renewable energy system (PV/Wind/PHS) under multiple constraints of connection to the electricity grid: A case study." *Wadi Alshatti Univ. J. Pure Appl. Sci.*, vol. 4, no. 1, pp. 83–93, 2026. https://doi.org/10.63318/waujpasv4i1_09
- [9] Y. Fathi, et al. "Feasibility of concentrating solar power as a solar fuel for electrical power stations: A case study of Ubari Gas-Power Station in Libya." *Wadi Alshatti Univ. J. Pure Appl. Sci.*, vol. 4, no. 1, pp. 56–69, 2026. https://doi.org/10.63318/waujpasv4i1_06
- [10] M. Khaleel, et al. "Optimum Number of Glass Covers of Thermal Flat Plate Solar Collectors." *Wadi Alshatti University Journal of Pure and Applied Sciences*, vol. 2, no. 1, pp. 1-10, 2024. <https://www.researchgate.net/publication/377082206>

- [11] A. Alkhazmi, et al. "Design and analysis of PV solar street lighting systems in remote areas: A case study," *Wadi Alshatti Univ. J. Pure Appl. Sci.*, vol. 4, no. 1, pp. 1–14, 2026, https://doi.org/10.63318/waujpasv4i1_01.
- [12] A. Al-Jamasi, et al. "Social awareness of the use of renewable energy among engineering college students at the Islamic University of Gaza, Palestine." *An-Najah Univ. J. Res. B (Humanities)*, vol. 36, no. 6, pp. 1173–1194, 2022. <https://doi.org/10.35552/0247-036-006-003>
- [13] F. El-Batta, and H. El-Khozondar, "Solar energy implementation at household in Gaza Strip," *Energy Sustain. Soc.*, vol. 12, pp. 12–17, 2022. <https://doi.org/10.1186/s13705-022-00343-7.z>
- [14] F. El-Batta, and H. Jarallah, "Solar energy as an alternative to conventional energy in Gaza Strip: Questionnaire-based study," *An-Najah Univ. J. Res. A (Nat. Sci.)*, vol. 32, no. 1, pp. 47–74, 2018. <https://doi.org/10.35552/anjr.a.32.1.1542>
- [15] A. Amhimmid, et al. "Financial modeling of social and environmental impacts of wind farm in urban zones: A case study of Zawia, Libya." *Int. J. Energy Environ. Eng.*, vol. 15, no. 4, pp. 1–20, 2024. <https://doi.org/10.57647/ijeee.2024.1504.17>
- [16] M. Albardawil, et al. "Sustainable street lighting in Gaza: Solar energy solutions for main street." *Energy 360*, vol. 4, p. 100042, 2025, <https://doi.org/10.1016/j.energy.2025.100042>
- [17] A. Ali, et al. "Economic and environmental implications of solar energy street lighting in urban regions: A case study." *Wadi Alshatti Univ. J. Pure Appl. Sci.*, vol. 3, no. 1, pp. 142–150, 2025. <https://www.researchgate.net/publication/390329694>
- [18] A. Alsharif, et al. "Photovoltaic solar energy for street lighting: A case study at Kuwaiti Roundabout, Gaza Strip, Palestine," *Power Eng. Eng. Thermophys.*, vol. 3, no. 2, pp. 77–91, 2024. <https://doi.org/10.56578/peet030201>
- [19] A. El Halim, et al. "DC off-grid PV system to supply electricity to 50 boats at Gaza Seaport," in *Proc. 8th Int. Eng. Conf. Renewable Energy & Sustainability (ieCRES)*, 2023. <https://doi.org/10.1109/ieCRES57315.2023.10209467>
- [20] K. Amer, et al. "Economic-Environmental-Energetic (3E) analysis of Photovoltaic Solar Energy Systems: Case Study of Mechanical & Renewable Energy Engineering Departments at Wadi AlShatti University." *Wadi Alshatti University Journal of Pure and Applied Sciences*, vol. 3, no. 1, pp. 51-58, 2025. https://doi.org/10.63318/waujpasv3i1_09
- [21] I. Imbayah, et al. "Design of a PV Solar-Covered Parking System for the College of Renewable Energy Tajoura, Libya: A PVsyst-Based Performance Analysis." *University of Zawia Journal of Engineering Sciences and Technology*, vol. 3, no. 2, pp. 288–307, 2025. <https://doi.org/10.26629/uzjest.2025.23>
- [22] H. Al-Najjar, et al. "Estimated view of renewable resources as a sustainable electrical energy source: Case study." *Designs*, vol. 4, no. 3, pp. 1–8. <https://doi.org/10.3390/designs4030032>
- [23] H. El-Khozondar and F. El-Batta. "Hybrid energy system for Deir El-Balah quarantine center in Gaza Strip, Palestine." in *Proc. Int. Conf. Electr. Power Eng.*, 2021. <https://doi.org/10.1109/ICEPE-P51568.2021.9423489>
- [24] C. Pfeifer, et al. "Microgrid for remote area in Gaza Strip powered by solar energy and olive oil mill waste." in *Sustainable Energy and Environmental Protection (SEEP)*, 2021. <https://www.researchgate.net/publication/356905648>
- [25] H. Al-Najjar, et al. "Performance evaluation of a hybrid grid-connected photovoltaic biogas-generator power system." *Energies*, vol. 15, p. 3151, 2022. <https://doi.org/10.3390/en15093151>
- [26] R. Al Afif, et al. "Implementation of maker movement to renewable energy laboratory: Case study of auto-tracking photovoltaic model." in *Proc. IEEE 7th Palestinian Int. Conf. Electr. Comput. Eng.*, 2019. <https://doi.org/10.1109/PICECE.2019.8747226>
- [27] C. Pfeifer, et al. "Solar energy powered toilet for emergency or remote areas usage." in *Proc. IEEE 7th Palestinian Int. Conf. Electr. Comput. Eng. (PICECE)*, Gaza, Palestine, Mar. 26–27, 2019. <https://doi.org/10.1109/PICECE.2019.8747168>
- [28] A. Aqila, N. Fathi, and S. Suliman. "Design of Hybrid Renewable Energy System (PV/Wind/Battery) Under Real Climatic and Operational Conditions to Meet Full Load of the Residential Sector: A Case Study of a House in Samno Village– Southern Region of Libya." *WAUJPAS*, vol. 3, no. 1, pp. 168-181, 2025. https://doi.org/10.63318/waujpasv3i1_23
- [29] E. Salim, A. Abubaker, B. Ahmed, and Y. Fathi. "A Brief Overview of Hybrid Renewable Energy Systems and Analysis of Integration of Isolated Hybrid PV Solar System with Pumped Hydropower Storage for Brack city - Libya." *Wadi Alshatti University Journal of Pure and Applied Sciences*, vol. 3, no. 1, pp. 152-167, 2025. https://doi.org/10.63318/waujpasv3i1_22
- [30] Y. Nassar, I. Latiwash, and A. Abubaker. "Performance Analysis and Sizing Optimization of a Utility Scale Stand-Alone Renewable Energy PV/Battery Storage System for Urban Zones." *University of Zawia Journal of Engineering Sciences and Technology*, vol. 3, no. 2, pp. 261–275, 2025. <https://doi.org/10.26629/uzjest.2025.21>
- [31] H. Jarallah, et al. "Standalone hybrid PV/wind/diesel-electric generator system for a COVID-19 quarantine center." *Environ. Prog. Sustain. Energy*, vol. 42, no. 3, p. e14049, 2023. <https://doi.org/10.1002/ep.14049>
- [32] F. El-Batta, et al. "Optimal design of a standalone hybrid energy system for a COVID-19 quarantine center." SSRN, 2021. <https://doi.org/10.2139/ssrn.3880850>
- [33] F. El-Batta, and H. J. El-Khozondar, "Survey study for the usage of solar energy at household by employees of Al-Shifa Medical Complex in Gaza Strip." *IOP Conf. Ser.: J. Phys.*, vol. 1108, p. 012125, 2018. <https://doi.org/10.1088/1742-6596/1108/1/012093>
- [34] Fathi, N., et al. "Atlas of Solar (PV and CSP) and Wind Energy Technologies in Libya." *International Journal of Electrical Engineering and Sustainability (IJEES)*, vol. 1, no. 3, pp. 27-43, 2023. <https://www.researchgate.net/publication/374846048>
- [35] Fathi, N. et al. "Mapping of PV Solar Module Technologies Across Libyan Territory." *Iraqi International Conference on Communication and Information Technologies*, pp. 227–232, Basrah, Iraq, 07-08 September 2022. <https://doi.org/10.1109/IICCIT55816.2022.10010476>
- [36] Miskeen, G., et al. "Atlas of PV solar systems across Libyan territory." *International Conference on Engineering & MIS (ICEMIS)*, Istanbul, Turkey, 04-06 July 2022, 10.1109/ICEMIS56295.2022.9914355
- [37] D. Albuzaia, A. Ali, M. Mohmed, and A. Hafez. "Reliable and Robust Optimal Interleaved Boost Converter Interfacing PhotoVoltaic Generator." *Wadi Alshatti University Journal of Pure and Applied Sciences*, vol. 3, no. 2, pp. 192-201, 2025. https://doi.org/10.63318/waujpasv3i2_24
- [38] A. Al-Mathnani, A. Mohammed, S. Al-Hashmi, and E. Geepalla. "Control and Modification of 12-Pulse Static Compensator with PV Cell Using New Control Algorithm." *Wadi Alshatti University Journal of Pure and Applied Sciences*, vol. 3, no. 1, pp. 30-34, 2025. https://doi.org/10.63318/waujpasv3i1_06
- [39] R Elzer, et al. "Assessing the Viability of Solar and Wind Energy Technologies in Semi-Arid and Arid Regions: A Case Study of Libya's Climatic Conditions." *Applied Solar Energy*, vol. 60, no. 1, pp. 149–170, 2024. <https://doi.org/10.3103/S0003701X24600218>
- [40] K. Matter, et al. "MATLAB/Simulink modeling to study the effect of partially shaded condition on photovoltaic array maximum power point." *Int. Res. J. Eng. Technol.*, vol. 2, no. 2, pp. 697–703, 2015. <https://www.researchgate.net/publication/322655620>
- [41] M. Elmnifi, et al. "Design and manufacture of a photovoltaic thermal solar collector equipped with aluminum foam fins for

- enhanced electrical, thermal, and integrated performance." *Heat and Mass Transfer*, vol. 173, no. 4, p. 110844, 2026. <https://doi.org/10.1016/j.icheatmasstransfer.2026.110844>
- [42] Y. Fathi, et al. "Thermoelectrical Analysis of a New Hybrid PV-Thermal Flat Plate Solar Collector." *2023 8th International Engineering Conference on Renewable Energy & Sustainability (ieCRES)*, Gaza, Palestine, State of, pp. 1-5, 2023. <https://doi.org/10.1109/ieCRES57315.2023.10209472>.
- [43] J. Halla, et al. "DC off-Grid PV System to Supply Electricity to 50 Boats at Gaza Seaport," *2023 8th International Engineering Conference on Renewable Energy & Sustainability (ieCRES)*, Gaza, Palestine, State of, pp. 1-5, 2023. <https://doi.org/10.1109/ieCRES57315.2023.10209467>.
- [44] K. Matter, et al. "Parameters influence on MPP value of the photovoltaic cell." *Energy Procedia*, vol. 74, pp. 1142–1149, 2015. <https://doi.org/10.1016/j.egypro.2015.07.756>
- [45] S. Alsadi, and Y. Nassar. "A general expression for the shadow geometry for fixed mode horizontal, step-like structure and inclined solar fields." *Solar energy*, vol. 181, pp. 53-69, 2019. <https://doi.org/10.1016/j.solener.2019.01.090>
- [46] A. Hafez, Y. Fathi, M. Hammdan, and S. Alsadi. "Technical and Economic Feasibility of Utility-Scale Solar Energy Conversion Systems in Saudi Arabia." *Iranian Journal of Science and Technology, Transactions of Electrical Engineering*, vol. 44, no. 1, pp. 213-225, 2019. <https://doi.org/10.1007/s40998-019-00233-3>
- [47] Y. Nassar, S. Alsadi, K. Ali, A. Yousef, and A. Massoud. "Numerical Analysis and Optimization of Area Contribution of The PV Cells in the PV/T Flat-Plate Solar Air Heating Collector." *Solar Energy Research Update*, vol. 6, pp. 43-50, 2019. <https://doi.org/10.31875/2410-2199.2019.06.5>
- [48] S. Alsadi. "Economical and environmental feasibility of the renewable energy as a sustainable solution for the electricity crisis in the Gaza Strip." Vol. 12, no. 3, pp. 35-44, 2016. <https://www.researchgate.net/publication/301328870>
- [49] K. Amer, et al. "Power Losses on PV Solar Fields: Sensitivity Analysis and a Critical Review." *International Journal of Engineering Research & Technology*, vol. 9, no. 9, pp. 1000-1007, 2020. <https://www.researchgate.net/publication/344520794>
- [50] Y. Fathi, and A. Salem. "The reliability of the photovoltaic utilization in southern cities of Libya ." *Desalination*, vol. 209, no. 1-3, pp. 86-90, 2007. <https://doi.org/10.1016/j.desal.2007.04.013>
- [51] Y. Nassar. *Solar energy engineering active applications*, Sebha University, Libya, 2006. <https://www.researchgate.net/publication/288670612>
- [52] A. Salem, et al. "The Choice of Solar Energy in the Field of Electrical Generation-Photovoltaic or Solar Thermal-For Arabic Region." *World Renewable Energy Congress VIII (WREC 2004)*, p. 534, 2004. <https://www.academia.edu/55830694/>
- [53] K. Osmani, et al. "A novel MPPT-based lithium-ion battery solar charger for operation under fluctuating irradiance conditions." *Sustainability*, vol. 15, no. 12, p. 9839, 2023. <https://doi.org/10.3390/su15129839>
- [54] E. Bayoumi, et al. "A smart energy monitoring system using ESP32 microcontroller." *J. Electr. Eng. Autom.*, vol. 6, no. 2, pp. 129–137, 2024. <https://doi.org/10.1016/j.prime.2024.100666>
- [55] O. Boucif, A. Lahoua, D. Boubiche, and H. Toral-Cruz, "Artificial intelligence of things for solar energy monitoring and control." *Appl. Sci.*, vol. 15, p. 6019, 2025. <https://doi.org/10.3390/app15116019>
- [56] L. Ben Dalla, O. Karal, M. EL-Sseid, and A. Alsharif. "An IoT-Enabled, THD-Based Fault Detection and Predictive Maintenance Framework for Solar PV Systems in Harsh Climates: Integrating DFT and Machine Learning for Enhanced Performance and Resilience." *Wadi Alshatti University Journal of Pure and Applied Sciences*, vol. 4, no. 1, pp. 41-55, 2026. https://doi.org/10.63318/waujpasv4i1_05
- [57] A. Mohammad, and F. Mahjabeen. "Revolutionizing solar energy: The impact of artificial intelligence on photovoltaic systems." *Int. J. Multidisciplinary Sci. Arts*, vol. 2, no. 1, pp. 117–127, Jun. 2023. <https://doi.org/10.47709/ijmdsa.v2i1.2599>
- [58] R. Belu. "Artificial intelligence techniques for solar energy and photovoltaic applications." in *Artificial Intelligence in Energy and Renewable Energy Systems*, S. A. Kalogirou, Ed. New York, NY, USA: Nova Publishers, pp. 376–436, 2013. <https://doi.org/10.4018/978-1-4666-1996-8.ch015>
- [59] A. Ahmed, and Y. Nassar. "AI-Powered Energy Forecasting: A Next-Gen Approach for Smart Grids and Sustainable Power Systems." *Eurasian Journal of Theoretical and Applied Sciences (EJTAS)*, vol. 1, no. 2, pp. 1-15, 2025. <https://doi.org/10.32213/w4zdxg34>
- [60] V. Umoh, J. Obot, and U. Ekpe. "Development of a smart solar energy management system." *Int. J. Adv. Res. Publ.*, vol. 3, no. 2, 2019. <https://www.researchgate.net/publication/340417735>
- [61] M. Habib, et al. "Automatic solar panel cleaning system based on Arduino for dust removal." in *Proc. Conf.*, 2021. <https://doi.org/10.1109/ICAIS50930.2021.9395937>
- [62] M. Osman, et al. "A comparative Analysis on Stacked Hybrid Intelligence: A Multi-Paradigm Machine Learning Framework for Robust Phishing URL Detection." *Comprehensive Journal of Science*, vol. 10, no. 39, pp. 1037-1062, 2026. <https://doi.org/10.65405/gcfgsj10>
- [63] S. Jumaboev, D. Jurakuziev, and M. Lee. "Photovoltaics plant fault detection using deep learning techniques." *Remote Sens.*, vol. 14, no. 15, p. 3728, 2022. <https://doi.org/10.3390/rs14153728>.
- [64] Z. Duranay. "Fault detection in solar energy systems: A deep learning approach." *Electronics*, vol. 12, no. 21, p. 4397, 2023. <https://doi.org/10.3390/electronics12214397>
- [65] A. Alatwi, et al. "Deep learning-based dust detection on solar panels: A low-cost sustainable solution for increased solar power generation." *Sustainability*, vol. 16, no. 19, p. 8664, 2024. <https://doi.org/10.3390/su16198664>
- [66] A. Kechida, et al. "Smart control and management for a renewable energy-based stand-alone hybrid system." *Sci. Rep.*, vol. 14, p. 32039, 2024. <https://doi.org/10.1038/s41598-024-83826-1>
- [67] U. Mamodiya, et al. "Artificial intelligence-based hybrid solar energy systems with smart materials and adaptive photovoltaics for sustainable power generation." *Sci. Rep.*, vol. 15, p. 17370, 2025. <https://doi.org/10.1038/s41598-025-01788-4>
- [68] A. Karthik, S. Mynampati, and P. Vairamoorthy. "Unified deep learning platform for dust and fault diagnosis in solar panels using thermal and visual imaging." *TechRxiv*, preprint, 2024. <https://doi.org/10.48550/arXiv.2511.18514>
- [69] D. Hosmer, S. Lemeshow, and R. Sturdivan., *Applied Logistic Regression*, 3rd ed. Hoboken, NJ, USA: Wiley, 2013.
- [70] C. Cortes, and V. Vapnik. "Support-vector networks." *Mach. Learn.*, vol. 20, no. 3, pp. 273–297, 1995. <https://doi.org/10.1007/BF00994018>
- [71] D. Rumelhart, G. Hinton, and R. Williams. "Learning representations by back-propagating errors." *Nature*, vol. 323, pp. 533–536, 1986. <https://doi.org/10.1038/323533a0>
- [72] Solar Panel Dust Detection Dataset, Kaggle, 2023. <https://www.kaggle.com/datasets/hemanthsai7/solar-panel-dust-detection>
- [73] R. Gonzalez, and R. Woods. *Digital Image Processing*, 4th ed. New York, NY, USA: Pearson, 2018. <https://www.cl72.org/090imagePLib/books/Gonzales,Woods-Digital.Image.Processing.4th.Edition.pdf>
- [74] A. Rahman. "Solar panel surface defect and dust detection: Deep learning approach." *J. Imaging*, vol. 11, p. 287, 2025. <https://doi.org/10.3390/jimaging11090287>
- [75] E. Almhdi, and G. Miskeen. "Power and Carbon Footprint Evaluation and Optimization in Transitioning Data Centres." *Wadi Alshatti University Journal of Pure and Applied Sciences*, vol. 4, no. 1, pp. 41-55, 2026. https://doi.org/10.63318/waujpasv4i1_05

- Applied Sciences*, vol. 3, no. 2, pp. 221-229, 2025. https://doi.org/10.63318/waujpasv3i2_28
- [76] S. Alfathi, G. Miskeen, and W. Mremi. "Evaluation and Prediction Performance of Solar Panel and Wind Turbine Systems Using Simulation." *Wadi Alshatti University Journal of Pure and Applied Sciences*, vol. 4, no. 1, pp. 94-104, 2026. https://doi.org/10.63318/waujpasv4i1_10